

## Solvent-Free Fabrication of Rare LaCO<sub>3</sub>OH Luminescent Superstructures

Vilas G. Pol,<sup>\*,†</sup> P. Thiyagarajan,<sup>†</sup> Jose M. Calderon Moreno,<sup>‡</sup> and Monica Popa<sup>‡</sup>

<sup>†</sup>IPNS, Argonne National Laboratory, Argonne, Illinois 60439, and <sup>‡</sup>Institute of Physical Chemistry Ilie Murgulescu, Romanian Academy, Spl. Independentei 202, Bucharest 060021, Romania

Received January 18, 2009

Lanthanum hydroxycarbonate (LaCO<sub>3</sub>OH) superstructures [LHS] decorated with carbon spheres are synthesized by a solvent-free, one-pot Reactions under Autogenic Pressure at Elevated Temperature (RAPET) process, dissociating a single lanthanum acetate hydrate (LAH) precursor. The structure of the as-synthesized LHS are studied by powder X-ray diffraction, high-resolution transmission electron microscopy, morphology by field-emission scanning electron microscopy, and the composition by energy dispersive X-ray analysis, elemental mapping, as well as FT-IR spectroscopy. The photoluminescence results showed an emission band centered at 465 nm ( $\lambda = \text{exc. } 360 \text{ nm}$ ) for the hexagonal phase of LHS. The mechanistic elucidation for the fabrication of LaCO<sub>3</sub>OH decorated with carbon spheres is developed on the basis of obtained thermal [TGA and DTA] data on initial LAH reactant.

### Introduction

Rare-earth materials have drawn much attention because of their wide range of applications in catalysis,<sup>1</sup> high-quality phosphors,<sup>2,3</sup> biological labeling<sup>4</sup> and magnetism.<sup>5</sup> However, most of the properties are dependent on the crystal type, shape, size, and composition. Among materials of the rare-earth family, lanthanum compounds with various morphologies have been synthesized, such as nanorods,<sup>6</sup> macropores,<sup>7</sup> and nanoplates<sup>8</sup> of La<sub>2</sub>O<sub>3</sub>; nanospheres,<sup>9</sup> nanowires,<sup>10</sup> and nanorods<sup>11</sup> of La(OH)<sub>3</sub>; spherical<sup>12</sup> La<sub>2</sub>(CO<sub>3</sub>)<sub>3</sub>; nanowires<sup>13,14</sup> of LaPO<sub>4</sub>; triangular nanoplates<sup>15</sup> and

flakes<sup>16</sup> of LaF<sub>3</sub>, etc. However, there is still much attention focused on the fabrication of novel lanthanum compounds because of their fluorescence properties, which originate from electron transitions within the 4f shell.

Lanthanum compounds doped with activated phosphors as a luminescent materials<sup>17</sup> have been widely studied. However, rare-earth hydroxycarbonates, especially LaCO<sub>3</sub>OH have been very rarely investigated. According to the comprehensive literature search, only few reports are found on the synthesis of LaCO<sub>3</sub>OH. LaCO<sub>3</sub>OH nanowires were synthesized by a solvothermal process controlling the volume ratio of ionic liquid (1,1,3,3-tetramethylguanidinium lactate) to water as the solvent.<sup>18</sup> Very recently, Zhang et al. synthesized LaCO<sub>3</sub>OH microspheres by a hydrothermal method using La(NO<sub>3</sub>)<sub>3</sub>·6H<sub>2</sub>O and urea CO(NH<sub>2</sub>)<sub>2</sub> as the starting materials. The 12 h hydrothermal<sup>19</sup> reactions were carried out in the temperature range of 210 to 270 °C after which the obtained precipitates were washed with distilled water followed by absolute ethanol several times and dried at 80 °C for 6 h. There are few additional reported efforts on the preparation of LaCO<sub>3</sub>OH. LaCO<sub>3</sub>OH was synthesized from hydrated lanthanum(III) carbonate<sup>20</sup> under hydrothermal conditions and by hydrolysis.<sup>21</sup> The treatment of lanthanum(III) nitrate or lanthanum(III) chloride<sup>22</sup> with urea or thiourea also yielded LaCO<sub>3</sub>OH. Additionally, the treatment of lanthanum(III) chloride with trifluoroacetic acid<sup>23</sup> or

- \*To whom correspondence should be addressed. E-mail: vilaspol@gmail.com.  
(1) Sun, C. W.; Sun, J.; Xiao, G. L.; Zhang, H. R.; Qiu, X. P.; Li, H.; Chen, L. Q. *J. Phys. Chem. B* **2006**, *110*, 13445.  
(2) Mai, H. X.; Zhang, Y. W.; Si, R.; Yan, Z. G.; Sun, L. D.; You, L. P.; Yan, C. H. *J. Am. Chem. Soc.* **2006**, *128*, 6426.  
(3) Wu, Y. Y.; Yan, H. Q.; Huang, M.; Messer, B.; Song, J. H.; Yang, P. D. *Chem.—Eur. J.* **2002**, *8*, 126.  
(4) Yi, G. S.; Lu, H. C.; Zhao, S. Y.; Ge, Y.; Yang, W. J.; Chen, D. P.; Guo, L. H. *Nano Lett.* **2002**, *2*, 733.  
(5) Lu, H. C.; Yi, G. S.; Zhao, S. Y.; Chen, D. P.; Guo, L. H.; Cheng, J. *J. Mater. Chem.* **2004**, *14*, 1336.  
(6) Wu, Q. Z.; Shen, Y.; Liao, J. F.; Li, Y. G. *Mater. Lett.* **2004**, *58*, 2688.  
(7) Tang, B.; Ge, J. C.; Wu, C. J.; Zhuo, L. H.; Niu, J. Y.; Chen, Z. Z.; Shi, Z. Q.; Dong, Y. B. *Nanotechnology* **2004**, *15*, 1273.  
(8) Si, R.; Zhang, Y. W.; You, L. P.; Yan, C. H. *Angew. Chem., Int. Ed.* **2005**, *44*, 3256.  
(9) Tang, B.; Ge, J. C.; Zhuo, L. H. *Nanotechnology* **2004**, *15*, 1749.  
(10) Wang, X.; Li, Y. D. *Angew. Chem., Int. Ed.* **2002**, *41*, 4790.  
(11) Wang, X.; Li, Y. D. *Chem.—Eur. J.* **2003**, *9*, 5627.  
(12) Jeevanandam, P.; Kolytipin, Y.; Palchik, O.; Gedanken, A. *J. Mater. Chem.* **2001**, *11*, 869.  
(13) Fang, Y. P.; Xu, A. W.; Song, R. Q.; Zhang, H. X.; You, L. P.; Yu, J. C.; Liu, H. Q. *J. Am. Chem. Soc.* **2003**, *125*, 16025.  
(14) Zhang, Y. J.; Guan, H. M. *Mater. Res. Bull.* **2005**, *40*, 1536.  
(15) Zhang, Y. W.; Sun, X.; Si, R.; You, L. P.; Yan, C. H. *J. Am. Chem. Soc.* **2005**, *127*, 3260.  
(16) Zhang, Y. J.; Hu, Q. X.; Guan, H. M.; Hu, B.; Fang, Z. Y.; Cheng, T.; Zhang, Z. D.; Chin, T. S. *J. Chem. Phys.* **2005**, *18*, 827.

- (17) Lehmann, O.; Kompe, K.; Haase, M. *J. Am. Chem. Soc.* **2004**, *126*, 14935.  
(18) Li, Z.; Zhang, J.; Du, J.; Gao, H.; Gao, Y.; Mu, T.; Han, B. *Mater. Lett.* **2005**, *59*, 963.  
(19) Zhang, Y.; Han, K.; Cheng, T.; Fang, Z. *Inorg. Chem.* **2007**, *46*, 4713.  
(20) Haschke, J. M. *J. Solid State Chem.* **1975**, *12*, 115.  
(21) Sun, J.; Kyotani, T.; Tomita, A. *J. Solid State Chem.* **1986**, *65*, 94.  
(22) Han, Z. H.; Yang, Q.; Lu, G. Q. *J. Solid State Chem.* **2004**, *111*, 3709.  
(23) Wakita, H.; Kinoshita, S. *Bull. Chem. Soc. Jpn.* **1979**, *52*, 428.

with sodium carbonate<sup>24</sup> leads to the formation of LaCO<sub>3</sub>OH.

Thus, considering the size and shape dependent significant luminescent properties of the LaCO<sub>3</sub>OH, developing other competitive methods for the fabrication of barely studied LaCO<sub>3</sub>OH is absolutely necessary. Consequently, we have developed a totally new approach based on thermolysis of a single chemical precursor in a controlled atmosphere that yields luminescent LaCO<sub>3</sub>OH with a novel morphology. The Reactions under Autogenic Pressure at Elevated Temperature (RAPET) of the LAH precursor in a closed reactor at 700 °C yielded LHS without using solvent or catalyst. The as-prepared LHS are systematically characterized to determine their morphology, structure, composition, and photoluminescence (PL) properties.

Previously, the RAPET process was successfully implemented to synthesize novel WC nanotubes,<sup>25</sup> WSe<sub>2</sub>,<sup>26</sup> high surface area SiC nanorods for hydrogen storage,<sup>27</sup> cathode nanomaterials for Li ion batteries,<sup>28</sup> MgB<sub>2</sub> nanoparticles with highest current density,<sup>29</sup> superconducting MgCNi<sub>3</sub>/C nanoflakes,<sup>30</sup> conducting silica-carbon nanocomposite<sup>31</sup> and paramagnetic carbons.<sup>32,33</sup> Recently, luminescent ZnO nanopencils<sup>34</sup> and ZnS/ZnSe nanopowders<sup>35</sup> were also prepared employing the RAPET approach. In those cases, either a single precursor with one metal or a mixture of different components were used; however, in none of the cases was hydroxycarbonate achieved in such distinctive morphology. Considering the possible applications of such rarely studied phosphors, efforts are made to select a smart precursor that will ease the synthesis of luminescent LaCO<sub>3</sub>OH in a simple, scalable, one pot process.

## Experimental Section

**1. Synthesis of LaCO<sub>3</sub>OH Superstructures Decorated with Carbon Spheres.** In a typical synthesis of LaCO<sub>3</sub>OH superstructures decorated with carbon spheres, 1.2 g of Lanthanum acetate hydrate [La(C<sub>2</sub>H<sub>3</sub>O<sub>2</sub>)<sub>3</sub>·xH<sub>2</sub>O] was introduced in a 5 mL reactor made up of Haynes 230 alloy at room temperature in an inert atmosphere. The inert reaction environment avoids the interference of other gases from the air, such as oxygen, CO<sub>2</sub>, and so forth. This control also facilitates the reproducibility of the fabrication of LaCO<sub>3</sub>OH. The partially filled reactor in an inert environment with precursor was placed at the center of a box furnace for uniform heating. The temperature of the furnace was ramped up to the desired temperature at a rate of 30 °C/min

and maintained at that temperature for 30 min. The reaction took place under the autogenic pressure formed during the course of the thermolysis of the precursor. **[Caution! For the safe operations, the chemical precursor(s) should not be loaded beyond the 25% of the reactors capacity.]** In the present case, the autogenic pressure created during the thermolysis of LAH precursor is recorded as 176 PSI at 700 °C. Although this is a minor pressure, it has a great impact on the growth of LaCO<sub>3</sub>OH. Upon natural cooling of the reactor to room temperature (~4 h), 0.81 g of gray powder is collected, characterized as LaCO<sub>3</sub>OH. Without further chemical processing, the as-prepared LHS product was analyzed for morphological, compositional, structural, and luminescence properties.

**2. Instrumental Details.** Phase purity and crystal structure of the obtained LHS material were determined using X-ray diffraction (XRD), and HR-TEM. The XRD pattern was recorded with a standard diffractometer (Model D5000 Siemens, Berlin, Germany) equipped with a graphite monochromator using Cu K $\alpha$  radiation ( $\lambda = 1.5405 \text{ \AA}$ ) operating at 40 mA and 40 kV, and employing a scanning rate of 0.02° and counting time of 5 s per step. The morphology of the thin films was observed by scanning electron microscopy (SEM) and transmission electron microscopy (TEM). SEM was performed using a Field-emission scanning electron microscope, JEOL JSM7500F, operated at the accelerating voltage of 15 kV. The TEM micrographs were recorded with a HITACHI HT800 apparatus equipped with a Link energy dispersive X-ray (EDX) system and operated at an accelerating voltage of 200 kV. The high resolution TEM and scanning transmission electron microscopy (STEM) micrographs with a JEOL 3011 Microscope operated at 300 kV equipped with a high angle annular dark field (HAADF) detector.

The LHS powder was ultrasonicated in ethanol, and a drop of the solution dried on a carbon coated microgrid for the TEM measurements. IR spectrum of LHS was obtained at a resolution of 2 cm<sup>-1</sup>, over the frequency range from 4000 to 400 cm<sup>-1</sup>, employing a Perkin-Elmer spectrophotometer. The spectrum was taken from thin (~20 mg/cm<sup>2</sup>) KBr pellets containing samples of approximately 1 wt %. The pellet was prepared by compacting an intimate mixture obtained by grinding 1 mg of substance in 100 mg KBr.

## Results and Discussion

For the fabrication of rare LaCO<sub>3</sub>OH, an initial RAPET reaction was carried out at 600 °C using LAH precursor. The as-prepared gray powder homogenized, out of which ~1 mg directly mounted on the double sided carbon tape supported on Si vapor. The sample for field emission scanning electron microscopy [FE-SEM] measurement was not coated with any additional conducting carbon or silver. The FE-SEM of the as-prepared LHS obtained after the thermolysis of LAH precursor in a closed reactor at 600 °C under autogenic pressure is presented in Figure 1. It can be seen that each superstructure of LaCO<sub>3</sub>OH is grown from an individual LAH, La(C<sub>2</sub>H<sub>3</sub>O<sub>2</sub>)<sub>3</sub>·xH<sub>2</sub>O particle [Figure 1a]. A high resolution micrograph [Figure 1b] demonstrates that the LaCO<sub>3</sub>OH plates are grown outward and assembled in a way to fabricate the rose-like flower morphology. Interestingly, completely spherical droplets (~1  $\mu\text{m}$  diameter particles) are observed decorating the surface of the plates. By selected area EDS analysis, these droplets are identified as the pure carbon. Overall, the grown luminescent flowers of LaCO<sub>3</sub>OH are mimicking the natural rose like morphology with water droplets on them. The close observation demonstrated that the plates are ~150 nm thick and several micrometers broad [Figure 1c]. The carbon spheres are physically bound on the

(24) Nagashima, K.; Wakita, H.; Mochizuki, A. *Bull. Chem. Soc. Jpn.* **1973**, *46*, 152.

(25) Pol, S. V.; Gedanken, A. *Adv. Mater.* **2006**, *18*, 2023.

(26) Pol, V. G.; Pol, S. V.; Calderon-Moreno, J. M.; Gedanken, A. *Phys. Chem. C* **2008**, *114*, 5356.

(27) Pol, V. G.; Pol, S. V.; Gedanken, A.; Lim, S. H.; Zhong, Z.; Lin, J. *J. Phys. Chem. B* **2006**, *110*, 11237.

(28) Odoni, A.; Pol, V. G.; Pol, S. V.; Aurbach, D.; Gedanken, A. *Adv. Mater.* **2006**, *18*, 1431.

(29) Pol, V. G.; Pol, S. V.; Felner, I.; Gedanken, A. *Chem. Phys. Lett.* **2006**, *433*, 115.

(30) Rana, R. K.; Pol, V. G.; Felner, I.; Meridor, E.; Frydman, A.; Gedanken, A. *Adv. Mater.* **2004**, *16*, 12.

(31) Pol, V. G.; Pol, S. V.; George, P. P.; Markovskiy, B.; Gedanken, A. *J. Phys. Chem. B* **2006**, *110*, 13420.

(32) Calderon-Moreno, J. M.; Crespo, D.; Battle, X.; Labarta, A.; Pol, V. G.; Pol, S. V.; Gedanken, A. *Carbon* **2006**, *44*, 2864.

(33) Pol, V. G.; Pol, S. V.; Markovskiy, B.; Calderon-Moreno, J. M.; Gedanken, A. *Chem. Mater.* **2006**, *18*, 1512.

(34) Pol, V. G.; Calderon-Moreno, J. M.; Thiyagarajan, P. *Langmuir* **2008**, *24*, 13640.

(35) Pol, S. V.; Pol, V. G.; Calderon-Moreno, J. M.; Cheylan, S.; Gedanken, A. *Langmuir* **2008**, *24*, 10462.

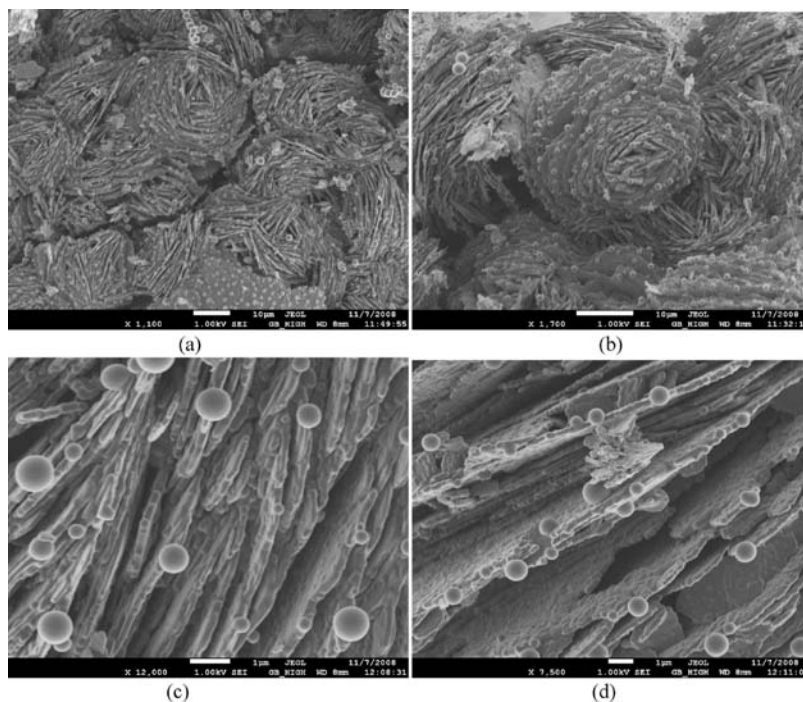


**Figure 1.** FE-SEM of the LHS obtained after the thermolysis of LAH precursor in a closed reactor at 600 °C under autogenic pressure; (a) low resolution SEM, (b) high resolution SEM, (c) standing  $\text{LaCO}_3\text{OH}$  plates, and (d) surface roughness of the  $\text{LaCO}_3\text{OH}$  plates.

$\text{LaCO}_3\text{OH}$  without getting detached during the powder mixing or SEM sample preparation. These complementary carbon spheres are formed in addition to  $\text{LaCO}_3\text{OH}$ , from the excess amount of carbon present in the precursor,  $\text{La}(\text{C}_2\text{H}_3\text{O}_2)_3 \cdot x\text{H}_2\text{O}$ . Additionally, it is noticed that the boundaries of the plates are zigzag. To recognize an exact morphology of the plates, a micrograph is taken with a different angle. A miniature roughness is recognized on the top surfaces of the plates [Figure 1d]. The plates are composed of  $\sim 100$  nm  $\text{LaCO}_3\text{OH}$  platelets causing surface roughness. The selected area EDS analysis complementary confirmed that these rough plates are of  $\text{LaCO}_3\text{OH}$  and not of carbon. It was hypothesized that an increase in the reaction temperature might merge the nanoplatelets to build a smoother plate. To verify this hypothesis, the RAPET of LAH is carried out at 700 °C, keeping the remaining analogous reaction conditions, and the morphologies of the achieved  $\text{LaCO}_3\text{OH}$  are presented in Figure 2.

At 700 °C, the overall corresponding flower-like morphology [Figure 2a,b] of  $\text{LaCO}_3\text{OH}$  is preserved as like in the reaction carried out at 600 °C. The flowers are grown outward originating from an individual LAH particles. The boundaries of the petals are zigzag even at 700 °C. The spherical carbon particles remained on the surfaces of the  $\text{LaCO}_3\text{OH}$  plates. [Figure 2c]. However, an anticipated change observed with increase in reaction temperature, namely, merging of the nanoplatelets [Figure 2d] to fabricate smoother surface of the plates. This might be due to Ostwald's ripening or presurface melting<sup>36</sup> of  $\text{LaCO}_3\text{OH}$  nanoplatelets at higher temperature under the pressurized system.

Although the morphological change (improved smoothness of the petal surfaces) with increase in reaction temperature

is recognized, this does not show any dramatic change in the structure, composition, or even on luminescence properties. Thus, only the representative HR-TEM characterization, XRD pattern, EDS analysis, IR data, and luminescence spectrum are presented for the  $\text{LaCO}_3\text{OH}$  prepared at 700 °C.

The further morphology and structure of the  $\text{LaCO}_3\text{OH}$  superstructures was studied dispersing the LHS powder in ethanol followed by ultrasonication and probing the small particles. Figure 3a shows the two-dimensional (2D) poly-dispersed plates of  $\text{LaCO}_3\text{OH}$ . The single plate at higher resolution is shown in Figure 3b. Since the flowers are grown outward until the available precursor, the plate does not show any unique size or shape. The selected area electro-diffraction pattern of one  $\text{LaCO}_3\text{OH}$  plate, Figure 3c, shows the hexagonal structure. Pattern indexing indicates that there is a preferential growth along the *ab* hexagonal plane.

The high resolution lattice images taken on an individual plate show a well ordered crystalline lattice [Figure 4], with a measured lattice plane distance of  $\sim 3.4$  Å. The atomic resolution images at higher magnification (Figure 4c,d) resolve atomic distances of 3.35 Å. The HR-TEM micrographs also revealed a non-perfect lattice, crystalline domains with different orientation in the hexagonal plane. Some grain boundaries can be clearly distinguished in Figure 4c, taken at the edge of the  $\text{LaCO}_3\text{OH}$  plate.

In Figure 5a, a typical XRD pattern of the  $\text{LaCO}_3\text{OH}$  powder obtained after the thermolysis of the LAH precursor in a closed reactor at 700 °C under autogenic pressure is presented. All of the reflection lines can be indexed to the hexagonal phase (JCPDS card 26-0815) with lattice constants

(37) Popa, M.; Kakihana, M. *Solid State Ionics* **2001**, *141*, 265.

(38) Popa, M.; Kakihana, M. *J. Therm. Anal. Calorim.* **2001**, *65*, 281.

(39) Hussein, G. A. M.; Buttrey, D. J.; DeSanto, P.; Abd-Elgaber, A. A.; Roshdy, H.; Myhoub, A. Y. Z. *Thermochim. Acta* **2003**, *402*, 27.

(36) Pol, V. G.; Gedanken, A.; Calderon-Moreno, J. M. *J. Nanosci. Nanotechnol.* **2005**, *5*, 975.

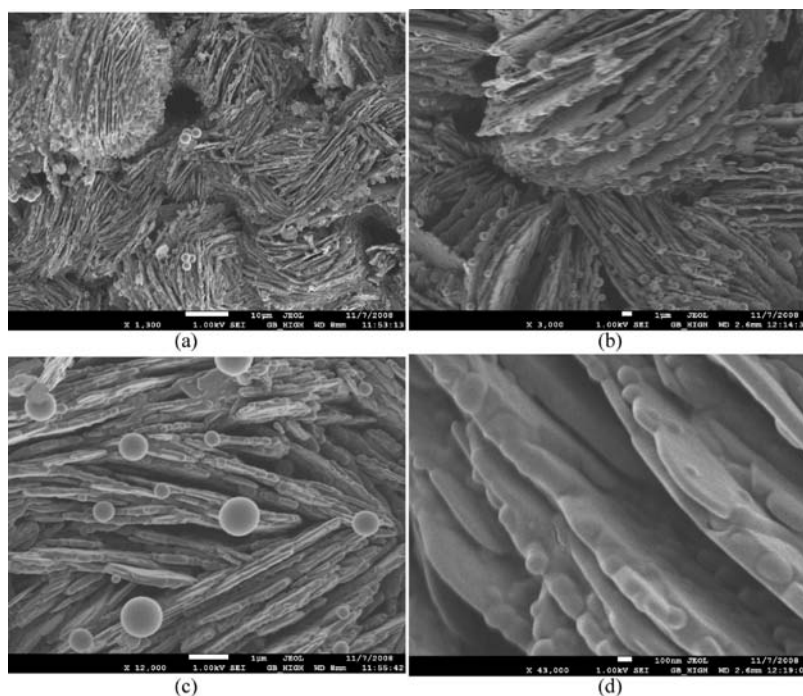


**Figure 2.** FE-SEM of the LHS obtained after the thermolysis of LAH precursor in a closed reactor at 700 °C under autogenic pressure; (a) low resolution SEM, (b) high resolution SEM, (c) standing  $\text{LaCO}_3\text{OH}$  plates, and (d) surface smoothness of the  $\text{LaCO}_3\text{OH}$ .

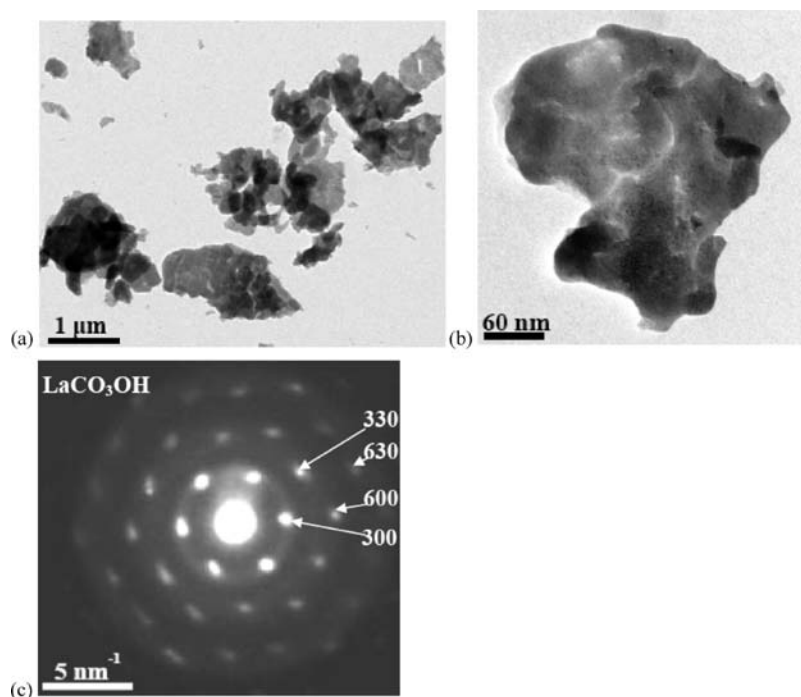


**Figure 3.** (a) Transmission electron micrograph of  $\text{LaCO}_3\text{OH}$ , (b) the TEM of single plate of  $\text{LaCO}_3\text{OH}$ , and (c) the electron diffraction pattern of  $\text{LaCO}_3\text{OH}$ .

$a = 1.261$  nm and  $c = 1.002$  nm. No other peaks exist in the pattern, confirming the crystallinity of the as-prepared  $\text{LaCO}_3\text{OH}$  sample. A similar XRD pattern was also reported by Li<sup>18</sup> and Zhang<sup>19</sup> et al. for hexagonal  $\text{LaCO}_3\text{OH}$ . The absence of carbon peaks is a signature of its poorly graphitic nature, supplementary information learned from Raman spectroscopy.

Additionally, the IR spectrum of  $\text{La}(\text{CO}_3)\text{OH}$  displayed quite strong bands between  $1520$  and  $1400$   $\text{cm}^{-1}$  and

$500$ – $1000$   $\text{cm}^{-1}$  [Figure 5b]. A similar IR pattern was also reported by Zhang<sup>19</sup> et al. for hexagonal  $\text{LaCO}_3\text{OH}$ . The weak absorptions displayed in the IR spectrum of  $\text{La}(\text{CO}_3)\text{OH}$  between  $3400$  and  $3700$   $\text{cm}^{-1}$  are due to the stretching mode of  $\text{OH}-\nu_{\text{OH}}$  at  $\sim 3615$  and  $\sim 3475$   $\text{cm}^{-1}$ , assigned to structural OH and adsorbed  $\text{H}_2\text{O}$ , respectively,<sup>19</sup> and the weak feature at  $683$   $\text{cm}^{-1}$  to the bending mode- $\delta_{\text{OH}}$  vibrations of water molecules. The additional weak bands at  $2360$  and  $667$   $\text{cm}^{-1}$  can be associated to the characteristic bands of

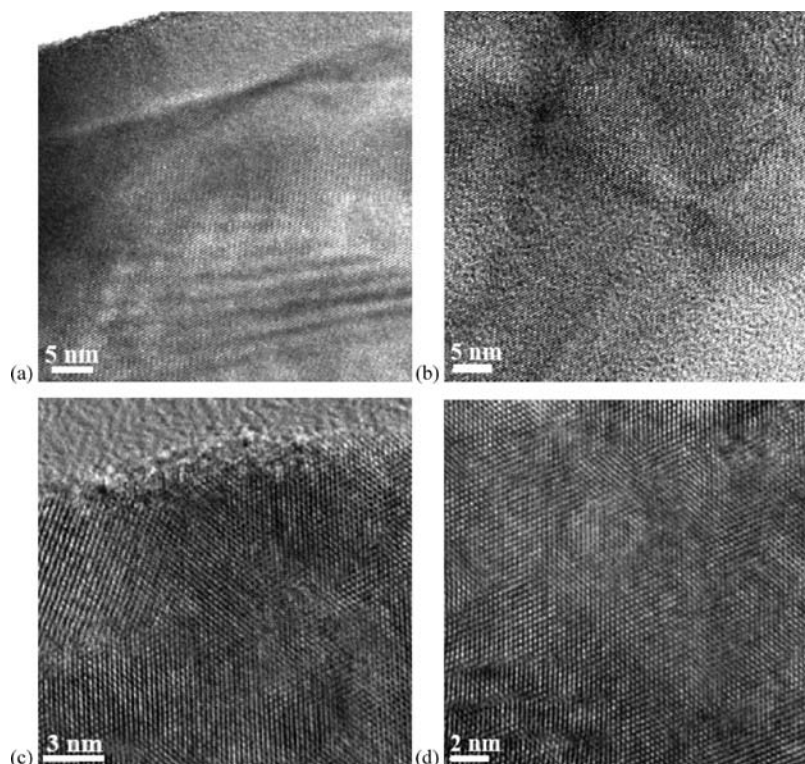


**Figure 4.** High resolution transmission electron micrographs of  $\text{LaCO}_3\text{OH}$  showing the lattice image (a, b) and atomic resolution images (c, d).

the deformation mode of gas phase of  $\text{CO}_2$ . The strong peaks at  $1400\text{--}1430\text{ cm}^{-1}$  are attributed to the carbonate  $\text{CO}_3^{2-}$  species,<sup>37–39</sup> at  $1430\text{ cm}^{-1}$  to the asymmetric vibrations frequency  $\nu_{\text{as}}(\text{COO}^-)$ , and at  $1400\text{ cm}^{-1}$  to the symmetric vibrations frequency  $\nu_{\text{s}}(\text{COO}^-)$ , respectively, while the band at  $1520\text{ cm}^{-1}$  might be from carboxylate groups. The minute bands are resolved [inset of Figure 5b] which appeared at  $872\text{--}845$  and  $705\text{ cm}^{-1}$  and are assigned to the  $\nu_4$  mode and the  $\nu_2$  bending mode of  $\text{CO}_3^{2-}$ , and the bands at  $790\text{--}774\text{--}754\text{ cm}^{-1}$  are probably due to the  $\delta_{(\text{COO})}$ -deformation vibrations. These observed very strong features in the spectrum of the  $\text{La}(\text{CO}_3)\text{OH}$  powders substantiate the claim that the plates are indeed composed of  $\text{La}(\text{CO}_3)\text{OH}$ .

Furthermore, EDS analysis evidenced that indeed the material is composed of La, C, and O [Figure 5c] without any additional elemental impurities. The EDS analysis measured the atomic % of La/C/O in the ratio of 1:3:4 in  $\text{LaCO}_3\text{OH}$  powder with minor deviations in various parts of the sample. For an exact formation of  $\text{LaCO}_3\text{OH}$  compound, the atomic % of La/C/O in the ratio of 1:1:4 is expected. The excess amount of carbon separately formed spherical particles and decorated the surface of the flowers as observed in the SEM. Here, the  $\text{LaCO}_3\text{OH}$  plates are grown first and the spherical carbons are settled on the surface in the later case because of its different thermodynamic stability.<sup>40</sup> The selected area EDS on a separate individual carbon sphere confirmed that the spherical decorated particles are composed of only carbon [Figure 5d]. The nature of the decorated carbon spheres is further investigated employing Raman spectroscopy in the  $1200\text{--}1700\text{ cm}^{-1}$  range. The peak at  $1347\text{ cm}^{-1}$  in the Raman spectrum [Figure 5e] is usually associated with the vibrations of carbon atoms with dangling

bonds for the in-plane terminated disordered graphite, labeled as the D-band.<sup>41,42</sup> The peak at  $1598\text{ cm}^{-1}$  (G-band) corresponding to the  $\text{E}_{2g}$  mode is closely related to the vibration of all the  $\text{sp}^2$ -bonded carbon atoms in a 2D hexagonal lattice, as in a graphene layer. The intensity ratio of the D and G bands (ID/IG) of 0.65 further quantifies that higher graphitic nature of the carbon spheres. The partial presence of disordered carbon is obvious since the growth temperature ( $700\text{ }^\circ\text{C}$ ) is not high enough to improve the long-range order of the newly formed graphite layers in the presence of  $\text{LaCO}_3\text{OH}$ .

The additional proof of the composition of  $\text{LaCO}_3\text{OH}$  is provided in the following La, O, and C elemental mapping on two separate 2D (Figure 6a–c), performed by EDS on the HAADF scanning transmission electron microscopy (STEM) image in Figure 6d. This further verified that the plates of  $\text{LaCO}_3\text{OH}$  are certainly composed of C, O, and La elements that further assemble to yield the superstructure.

To understand the mechanistic elucidation for the formation of natural flower like growth of  $\text{LaCO}_3\text{OH}$ , the thermal gravimetric [Figure 7a] and differential thermal [Figure 7b] analysis of the LAH precursor was carried out in an inert argon atmosphere. In the TGA, the weight losses in three steps are recorded during the thermolysis of LAH. The first 4% weight loss at  $\sim 100\text{ }^\circ\text{C}$  is due to water loss from the LAH precursor, the corresponding endothermic peak is recorded above  $100\text{ }^\circ\text{C}$  in DTA. The small exotherm at  $200\text{ }^\circ\text{C}$  in DTA evidenced that LAH might have started degrading. In between  $300$  and  $400\text{ }^\circ\text{C}$ , further 40% weight loss is recorded in

(41) Dresselhaus, M. S.; Dresselhaus, G.; Pimenta, M. A.; Eklund, P. C. In *Analytical applications of Raman spectroscopy*; Pelletier, M.J., Ed.; Oxford: Blackwell, 1999; Chapter 9.

(42) Pol, V. G.; Calderon-Moreno, J. M.; Chupas, P. J.; Winans, R. E.; Thiyagarajan, P. *Carbon* **2009**, *47*, 1050.

(40) Pol, S. V.; Pol, V. G.; Gedanken, A. *Chem.—Eur. J.* **2004**, *10*, 4467.

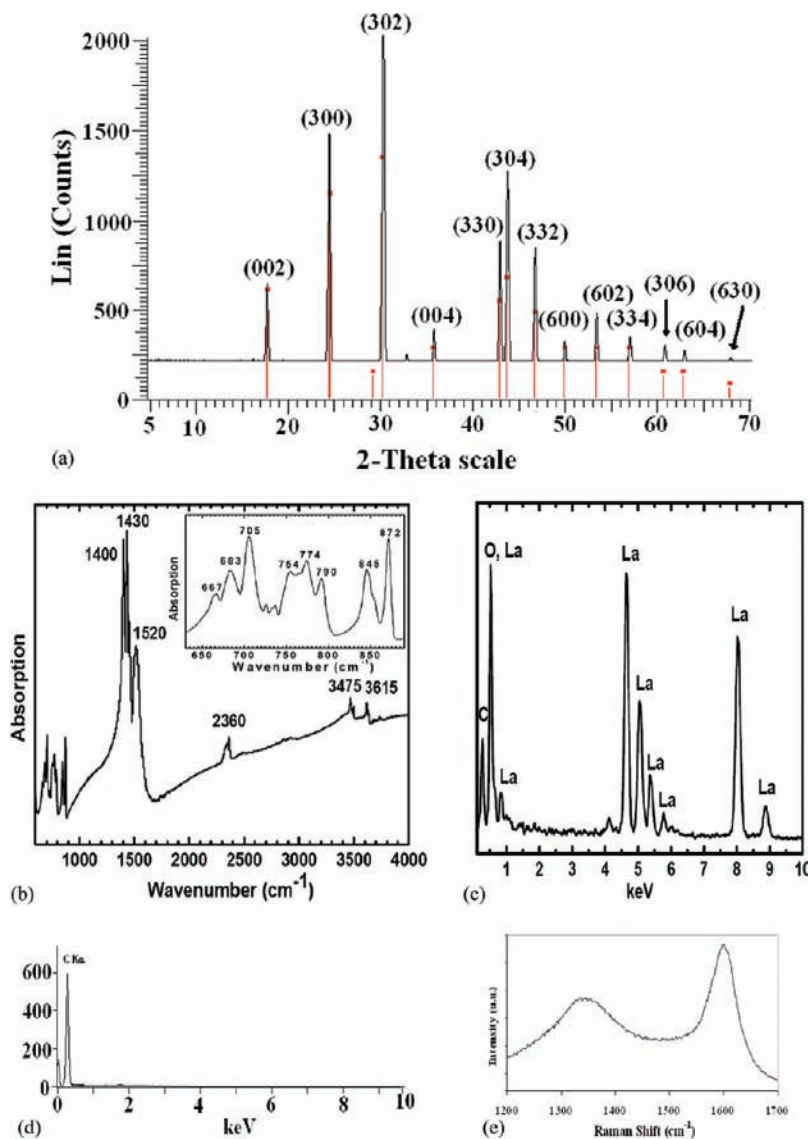
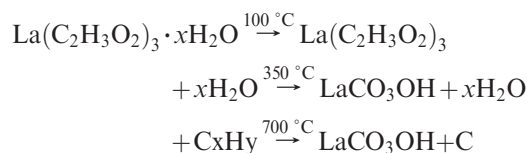


**Figure 5.** (a) Powder-XRD pattern (the tiny peak at 33 degree is from the sample holder), (b) FT-IR (the inset shows the magnified low wavenumber region), (c) energy dispersive X-ray analysis of the LHS obtained after the thermolysis of LAH precursor in a closed reactor at 700 °C under autogenic pressure, (d) selected area EDS on spherical carbon bodies, and (e) Raman spectrum in the range of carbon bands.

the TGA, while the exotherm is recorded in the DTA. This is an indication for the conversion of  $\text{La}(\text{C}_2\text{H}_3\text{O}_2)_3$  into  $\text{LaCO}_3\text{OH}$ . Our XRD, HR-TEM, IR, EDS, and elemental mapping supported that the plates are made up of  $\text{LaCO}_3\text{OH}$ . The TGA cooling (not shown) and DTA cooling cycles are featureless. The third 4% weight loss might be due to combustion of carbon in the TGA. These changes all happened during the thermolysis of the LAH precursor in the flowing inert atmosphere. The following reaction is anticipated considering the acquired thermal data.



The present RAPET decomposition of LAH is carried out in an inert atmosphere in a closed reactor that facilitated the flower-like  $\text{LaCO}_3\text{OH}$  product at higher temperature.

Although the reaction might complete at lower temperature, to gain the luminescence from crystalline  $\text{LaCO}_3\text{OH}$ , we carried out RAPET reactions at 600 and 700 °C. Additionally, water vapors and carbonaceous products created autogenic pressure at high temperature, which plays an important role in the growth of flower-like superstructures. It is worth noting that a controlled reaction where LAH was heated in air atmosphere yielded micrometer size  $\text{La}_2\text{O}_3$  with poly dispersed morphology. The autogenic pressure created during the thermolysis of LAH is recorded as 176 PSI at 700 °C. For the in situ measurement of an autogenic pressure at high temperature, a separate set up is developed and demonstrated elsewhere.<sup>43</sup>

In the present case, the gathering of the initially formed  $\text{LaCO}_3\text{OH}$  particles is a result of the RAPET reaction conditions (temperature, pressure, solid product, and gases in a closed reactor). It is believed that under such conditions the  $\text{LaCO}_3\text{OH}$  crystal is polar whose positive polar plane is

(43) Pol, V. G.; Thiyagarajan, P. *Ind. J. Chem. Res.* **2009**, *48*, 1484.

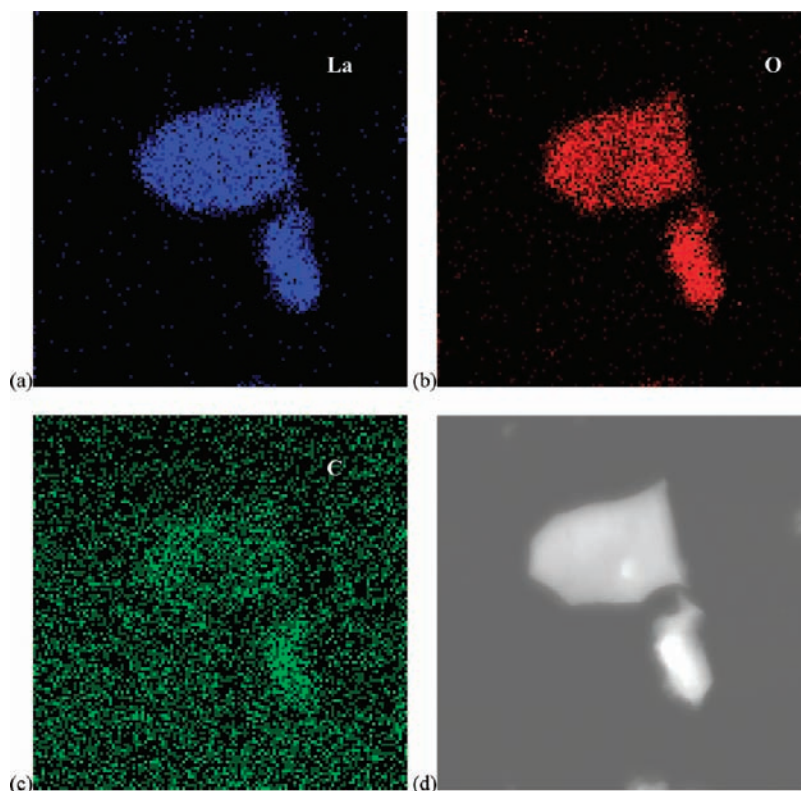


**Figure 6.** EDS elemental mapping of (a) La, (b) O, (c) C on two separate 2D plates, and (d) the corresponding HAADF scanning transmission electron microscopy (STEM) image.

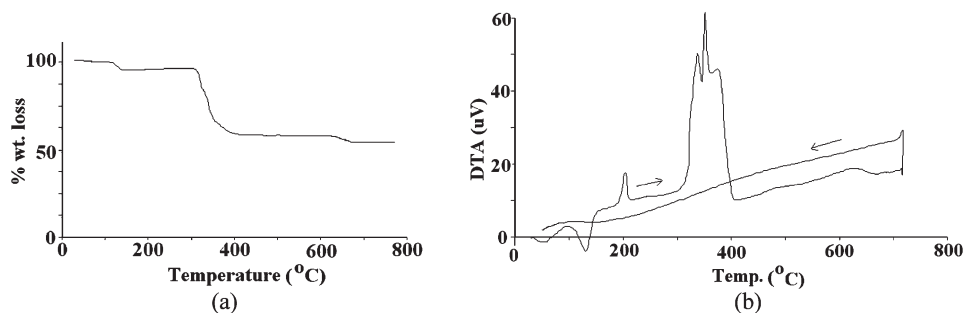


**Figure 7.** (a) Thermo-gravimetric analysis and (b) differential thermal analysis of LAH precursor in inert atmosphere.

rich in La and the negative polar plane is rich in OH/CO<sub>3</sub>. The growth mechanism is recently reported for the faceted and prismatic polar ZnO pencils with hexagonal crystal structure after the dissociation of zinc acetate dihydrate under the autogenic pressure at elevated temperature.<sup>35</sup> According to the mechanism described by Zhang et al. for the synthesis of LaCO<sub>3</sub>OH microspheres,<sup>19</sup> when the overall growth rate is fast, the anisotropic growth of the material is expected. On the contrary, if the overall growth rate is slow, a nearly spherical morphology is favored in their case where the reaction was carried out for 12 h. In fact the growth of present LaCO<sub>3</sub>OH flowers is carried out within 30 min of reaction, which is favored to grow plates faster in a specific direction because of its polar nature. This hypothesis is also tested by changing the reaction times, keeping analogous reaction conditions. Indeed, the growth of the LaCO<sub>3</sub>OH crystal was initiated when the reaction time was 5 min, while negligible effect was observed when the reaction time was greater than 30 min. Thus, rapid growth of bidimensional plates by coalescence of nanocrystallites via Ostwald ripening<sup>36</sup>

phenomena yielded LaCO<sub>3</sub>OH superstructures. We also noticed sintering and growth mechanism of the nanocrystallites in SEM and in HR-TEM measurements. In comparison with low temperature routes, the high temperature and reactive media (dense due to high pressure, and in a reductive environment) is critical to allow the sintering of nanocrystallites at the same time that the crystallites are being nucleated, until the depletion of the source, leading to growth of bidimensional plates and flower-like superstructures.

Since the LaCO<sub>3</sub>OH is rarely prepared, the optical properties of such rare-earth compounds have hardly ever been investigated until now. The room temperature excitation (Figure 8a) and PL (Figure 8b) spectra are shown for the LHS prepared at 700 °C. The emission spectrum has only one broadband centered on 465 nm with the 360 nm excitation, without using a filter. It is known that the fluorescence of rare-earth ions mainly comes from the interior electron transitions of the 4f shell,<sup>44</sup> but the 4f shell of La<sup>3+</sup> is empty

(44) Huo, Z. Y.; Chen, C.; Li, Y. D. *Chem. Commun.* **2006**, 33, 3522.

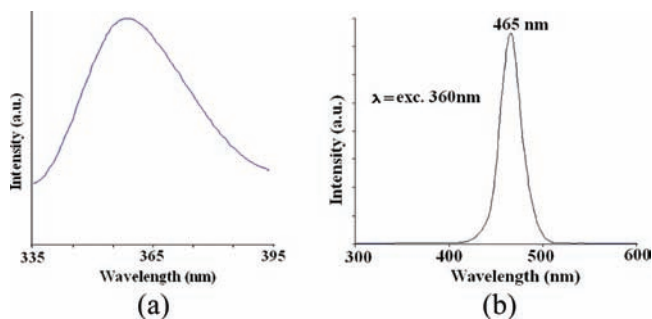


**Figure 8.** Excitation (a) and PL (b) spectra of the LHS at room temperature.

and no f-f transitions exist in the  $\text{LaCO}_3\text{OH}$  powder. Herein, the emission spectrum of the  $\text{LaCO}_3\text{OH}$  powder consists of a broadband located between 400 and 520 nm and can be attributed to the self-trapped exciton (STE) luminescence.<sup>45</sup> Many of the free holes and free electrons were created after the lattice was irradiated, and the STEs can be formed directly from electron–hole pairs. During the diffusion of the STEs, there can be an irradiative recombination, leading to luminescence,<sup>46</sup> and the possible origin of the visible PL. Zhang et al. reported the PL of  $\text{LaCO}_3\text{OH}$  microspheres at

(45) Chen, F.; Liu, H. W.; Wang, K. F.; Yu, H.; Dong, S.; Chen, X. Y.; Jiang, X. P.; Ren, Z. F.; Liu, J. M. *J. Phys.: Condens. Matter* **2005**, *17*, L467.

(46) Kawabe, Y.; Yamanaka, A.; Hanamura, E.; Kimura, T.; Takiguchi, Y.; Kan, H.; Tokura, Y. *J. Appl. Phys.* **2000**, *87*, 7594.

438 nm,<sup>19</sup> while our recorded PL is centered at 465 nm. This red shift might be due to the decorated carbon spheres on the surfaces of the present  $\text{LaCO}_3\text{OH}$  superstructures. An analogous effect was observed in the case of ZnO pencils<sup>35</sup> coated with carbon spheres. The noticed red shift is due to oxygen deficiency created during the reducing atmosphere of carbon in the reaction.

## Conclusions

The one-pot, solvent-less synthesis process for the fabrication of PL  $\text{LaCO}_3\text{OH}$  powder is demonstrated from the thermal dissociation of the LAH single precursor. The structure of the as-synthesized  $\text{LaCO}_3\text{OH}$  powder is studied by powder XRD, HR-TEM, morphology by FE-SEM, and the composition by EDS, elemental mapping, as well as FT-IR spectroscopy. The green emission band centered at 465 nm for the  $\text{LaCO}_3\text{OH}$  superstructures decorated by carbon spheres is recorded using 360 nm excitation wavelength. The growth mechanism for the fabrication of  $\text{LaCO}_3\text{OH}$  flowers is developed on the basis of thermal [TGA and DTA] data obtained for the initial LAH precursor.

**Acknowledgment.** Use of the Center for Nanoscale Materials was supported by the U.S. Department of Energy, Office of Science, Office of Basic Energy Sciences, under Contract No. DE-AC02-06CH11357. Authors thanks to Dr. Elena Shevchenko for providing assistance to the FE-SEM measurements.